Interpreting eddy fluxes

Carsten Eden[1], Richard J. Greatbatch[2] and Dirk Olbers[3]

[1] *Leibniz-Institut für Meereswissenschaften, IFM-GEOMAR, Kiel, Germany*

[2] *Department of Oceanography, Dalhousie University, Halifax, Canada*

[3] *Alfred Wegener Institute for Polar and Marine Research, Bremerhaven, Germany*

Manuscript submitted in final form to JPO, August 2006.

Corresponding author address:
Carsten Eden
IFM-GEOMAR,
FB I, Ocean circulation and climate dynamics
Düsternbrooker Weg 20
24105 Kiel, Germany
email: ceden@ifm-geomar.de

All figures are available in electronic format.

Abstract

A generalisation of the Transformed Eulerian and Temporal Residual Means is presented. The new formulation uses rotational fluxes of buoyancy, and the full hierarchy of statistical density moments, to reduce the cross-isopycnal eddy flux to the physically relevant component associated with the averaged water mass properties. The resulting eddy-induced diapycnal diffusivity vanishes for adiabatic, statistically steady flow, and is related to either growth or decay of mesoscale density variance and/or the covariance between small-scale forcing (mixing) and density fluctuations, such as associated with the irreversible removal of density variance by dissipation. The relationship between the new formulation and previous approaches is described, and illustrated using results from an eddying channel model. The formalism is quite general and applies to all kinds of averaging and to any tracer (not just density).

1 Introduction

The Boussinesq form of the conservation equation for a tracer with concentration b in the ocean (or the atmosphere) is given by

$$\frac{\partial b}{\partial t} + \nabla \cdot (\boldsymbol{u} b) = Q \tag{1}$$

where $\boldsymbol{u}$ denotes the instantaneous, three-dimensional velocity and Q a forcing term. Both the ocean and atmosphere are turbulent fluids, full of "rapidly evolving perturbations" (eddies) on a "slowly evolving mean state". The presence of the eddies means that the instantaneous tracer distribution is often of little interest; instead, it is the dynamics and evolution of an "averaged" state which is important. This, in turn, requires the definition of an average or filter with which to view the dynamics and evolution of the tracer field, and which, in turn, determines what is meant by "rapid", "slow" and "mean state".

A simple example is the zonal mean; that is b, $\boldsymbol{u}$ and Q are decomposed into zonal averages at constant height and deviations from that average:

$$\bar{b} = (x_2 - x_1)^{-1} \int_{x_1}^{x_2} b \, dx \quad , \quad b' = b - \bar{b} \tag{2}$$

and correspondingly for $\boldsymbol{u}$ and Q. Substituting the decomposition given by Eq. (2) into the instantaneous tracer budget and averaging the result leads to the equation for the mean tracer $\bar{b}$ given by

$$\frac{\partial \bar{b}}{\partial t} + \nabla \cdot (\bar{\boldsymbol{u}} \bar{b}) + \nabla \cdot (\overline{\boldsymbol{u}' b'}) \quad = \quad \bar{Q} \tag{3}$$

An immediate difficulty is presented by the eddy tracer flux[1] $\overline{\boldsymbol{u}' b'}$. These fluxes couple the mean tracer budget to that of the perturbations, such that the evolution of the perturbations has to be known to predict the mean tracer. Of course, the solution to this problem is thought to be given by parameterising the perturbation quantities in terms of the mean quantities. However, before parameterising the effect of the eddy tracer fluxes, it is necessary to understand and

[1] Note that the vectors $\bar{\boldsymbol{u}}$, $\boldsymbol{u}'$, the operator ∇ and correspondingly the fluxes $\bar{\boldsymbol{u}}\bar{b}$ and $\overline{\boldsymbol{u}' b'}$ in Eq. (2) and in the following section are two dimensional, that is their zonal component vanishes.

interpret them. Understanding and interpreting the eddy fluxes is the focus of the present paper.

Some insight into the nature of the eddy tracer flux can be obtained by considering a layered framework, in which instantaneous contours of b are taken as layer interfaces. In the continuous limit of infinitesimal layer thickness, this is the same as using b as the vertical coordinate[2]. Taking b to be potential density[3] then corresponds to using "isopycnal coordinates" (e.g. McDougall (1987)). Since the interior oceanic flow is almost adiabatic (Wüst, 1935), the diabatic forcing Q is expected to be small in the ocean interior and to be associated with weak diapycnal mixing. In the limit of vanishing instantaneous forcing Q, there is no instantaneous exchange of b across layers (isopycnals) and it is easy to see that in the isopycnally-averaged budget for b there can be no cross-isopycnal flux. Furthermore, the mean forcing (related to Q) is controlling the cross-isopycnal flux in the mean budget of the layer thickness.

Returning to z-coordinates, this property of the eddy fluxes is not as obvious. In fact, eddy tracer fluxes averaged at constant height (instead of at constant b) usually show strong cross-isopycnal components even for the steady, weakly diabatic case, suggesting strong, apparently eddy-induced diapycnal processes as we shall show below. On the other hand, z-coordinates are convenient and simple to use for both analytical considerations and numerical calculations. In fact, an overwhelming number of analytical and numerical models are based on z-coordinates, rather than layered or isopycnal coordinates.

Therefore, it would be desirable if the character of eddy tracer fluxes as revealed above in the layered framework could be carried over to the mean tracer budget in z-coordinates. Based on these considerations, we can formulate the following statement, which we would like to apply in quasi-steady[4] conditions in z-coordinates:

i) If there is locally no diabatic forcing, Q, in the instantaneous tracer budget Eq. (1), there

[2]Assuming that b is a monotonic function of depth. See Nakamura (2001) and Nurser and Lee (2004) for a generalisation of this approach for non-monotonic functional forms of b.

[3]Note that we assume for simplicity an equation of state in which potential density and neutral density are the same.

[4]We mean by quasi-steady state that $\frac{\partial \bar{b}}{\partial t} = 0$ but, in general, $\frac{\partial b'}{\partial t} \neq 0$.

should be locally also no diabatic effects in the *mean* budget Eq. (3). As a consequence, the divergence of the eddy tracer flux $\overline{\boldsymbol{u}'b'}$, must be entirely expressible as a divergence of an advective flux of the mean tracer.

For non-zero Q, on the other hand, we expect there to be diabatic effects due to the eddies that are contained in the divergence of $\overline{\boldsymbol{u}'b'}$ in the budget for $\bar{b}$. The diabatic nature of the eddy fluxes can be understood in an integral sense in z-coordinates as outlined by Radko and Marshall (2004).

Consider an integral over an area A (or volume for the three-dimensional case and temporal averaging) above a mean isopycnal $\bar{b}(y,z) = const$ of the mean tracer budget Eq. (3) in, for instance, a cross section of a channel

$$\int_A dA(\nabla \cdot (\bar{\boldsymbol{u}}\bar{b}) + \nabla \cdot (\overline{\boldsymbol{u}'b'})) = \int_A dA(\bar{Q} - \frac{\partial}{\partial t}\bar{b}) \tag{4}$$

Using Gauss' divergence theorem and the no flow boundary conditions for the mean and the eddy tracer fluxes at the northern and southern lateral boundaries of the channel and the surface, it is clear that only the eddy flux across the mean isopycnal $\bar{b} = const$ remains from the mean and eddy advection in the integral balance:

$$\int_{s_0}^{s_1} \overline{\boldsymbol{u}'b'} \cdot \boldsymbol{n}\, ds = \int_A dA(\bar{Q} - \frac{\partial}{\partial t}\bar{b}) \tag{5}$$

where the vector $\boldsymbol{n} = \nabla\bar{b}|\nabla\bar{b}|^{-1}$ points perpendicular to the mean isopycnal $\bar{b} = const$ and s denotes a coordinate along the mean isopycnal from s_0 at the southern end of the channel to s_1 at the northern end of the channel. This means that if the integral on the right hand side of the integral balance vanishes, i. e. if the mean diapycnal forcing $\bar{Q}$ vanishes in quasi-steady state, the integrated diapycnal eddy flux across the mean isopycnal must also vanish.

Eq. (5) therefore yields an integral constraint for averaging in z-coordinates, similar to the previous one averaging in isopycnal coordinates. The difference is that the constraint in z-coordinates holds only in a (weaker) integral sense while in isopycnal coordinates the constraint holds also locally. That means that statement i), which was deduced from the

isopycnal framework and applied to z-coordinates, carries over the weaker integral constraint to a (stronger) local one in z-coordinates.

The way we shall implement statement i) in this paper is by taking account of rotational fluxes in an eddy flux decomposition into advective and diffusive parts, similar to the flux decompositions of Andrews and McIntyre (1978) and McDougall and McIntosh (1996). As examples of the performance of our eddy flux interpretation we diagnose numerical experiments, which are presented in section 2. In section 3, we review the classical flux decomposition by Andrews and McIntyre (1978), the Transformed Eulerian Mean (TEM) method, and diagnose it in the numerical experiments. Section 4 presents a TEM version, which was originally proposed by Gille and Davis (1999) and which is equivalent to the effective diffusivity concept by Nakamura (2001). However, while all these TEM versions are shown to be inconsistent with statement i), in section 5 we finally discuss and apply to the model a consistent and satisfactory generalisation of the eddy flux interpretations of Marshall and Shutts (1981); McDougall and McIntosh (1996) and Medvedev and Greatbatch (2004). The last section concludes and discusses the results.

2 Numerical simulations of eddy fluxes

We are diagnosing numerical experiments using an OGCM in several idealised configurations with respect to several eddy flux decompositions. The numerical code[5] which is used to integrate the OGCM is based on a revised version of MOM2 (Pacanowski, 1995) and formulated in z-coordinates.

Experiment CHANNEL-3 is a setup with a reentrant channel on a β-plane (referenced to the southernmost latitude of the model domain). Horizontal resolution is $1/3^o$ and there are 20 levels of 100 m thickness. Initial conditions are a state of rest and constant meridional and vertical gradients in temperature ($-1 \times 10^{-5} K/m$ and $8.2 \times 10^{-3} K/m$ respectively) and no

[5]The numerical code together with all configurations used in this study can be accessed at *http://www.ifm.uni-kiel.de/fb/fb1/tm/data/pers/ceden/spflame/index.html*.

zonal gradient (except for a small perturbation). A linear equation of state is used ($\partial\rho/\partial T = -0.2 \times 10^{-3} kg/m^3/K$) and salinity set to a constant. Boundary conditions are no slip at the side walls and vanishing heat fluxes at the side walls, surface and bottom boundaries. Bottom friction following a quadratic drag law is used with a coefficient of 1.5×10^{-3}, lateral biharmonic friction with viscosity of $2 \times 10^{11} m^4/s$ and the Quicker advection scheme (Leonard, 1979) for the tracer with no explicit diffusion. Explicit vertical viscosity is $2 \times 10^{-4} m^2/s$. Temperature at the three northernmost and southernmost grid points is relaxed towards the initial condition with a timescale ranging from 3 days at the boundary to 15 days at the outer edge of the relaxation zone.

Two further experiments are discussed in which we aim to reduce the interior diabatic forcing. Since we use no explicit diffusion in all model runs, the diabatic forcing outside the relaxation zones is due to implicit (numerical) diffusion by the advection scheme (Quicker) and other spurious numerical effects (Griffies et al., 2000; Eden and Oschlies, 2006). The most effective way to reduce these effects and correspondingly Q in the model is simply given by increasing the resolution. In experiment CHANNEL-6 (CHANNEL-12) the horizontal and vertical model resolution was increased by a factor 2 (4). In addition, the biharmonic viscosity was decreased to $1 \times 10^{11} m^4/s$ ($2 \times 10^{10} m^4/s$) and the temperature is relaxed towards the initial condition in 6 (12) southern- and northernmost grid points. All other aspects of the model are unchanged with respect to experiment CHANNEL-3.

After a couple of weeks of simulation time, baroclinic instability sets in and is producing large zonal deviations of the flow in the channel in all experiments. Figure 1 shows the fully developed stage of turbulence after one year integration in CHANNEL-3. In all experiments, the model is integrated for 40 years and temporal and zonal averages are taken for the last 30 years of the integration. In the following we relate b to temperature, i. e. density, since temperature acts as the only (active) tracer in the model.

3 The classical eddy flux decomposition

In this section we review the classical way of interpreting the eddy tracer flux resulting from zonal averaging at constant height. Note that all results carry over to temporal averaging in three dimensions. Note also that we use the following notation (Hasselmann, 1982)

$$\nabla\alpha = \begin{pmatrix} \alpha_y \\ \alpha_z \end{pmatrix} \quad \text{and} \quad \underset{\neg}{\nabla}\alpha = \begin{pmatrix} -\alpha_z \\ \alpha_y \end{pmatrix} \tag{6}$$

where the subscripts y and z denote differentiation of the scalar α in the meridional and vertical direction, respectively, and the vector subscript $\neg$ anti-clockwise rotation by 90^o.

The Transformed Eulerian Mean method of Andrews and McIntyre (1978) (TEM hereafter) introduces a decomposition of the eddy tracer flux $\boldsymbol{F}$ into a part aligned along contours of $\bar{b}$ and a part across contours of $\bar{b}$

$$\overline{\boldsymbol{u}'b'} \equiv \boldsymbol{F} \;\; = \;\; B\,\underset{\neg}{\nabla}\bar{b} - K\nabla\bar{b} \tag{7}$$

where B and K are given by projections of the eddy flux along and across contours of $\bar{b}$ respectively

$$B \;\; = \;\; |\nabla\bar{b}|^{-1}F_{||} \tag{8}$$

$$K \;\; = \;\; -|\nabla\bar{b}|^{-1}F_{\perp} \tag{9}$$

with $F_\perp = \overline{\boldsymbol{u}'b'}\cdot\boldsymbol{n}$ the cross-isopycnal component of the eddy tracer fluxes, $F_{||} = \overline{\boldsymbol{u}'b'}\cdot\boldsymbol{s}$ the along-isopycnal component of the eddy tracer fluxes, and where $\boldsymbol{s} = |\nabla\bar{b}|^{-1}\,\underset{\neg}{\nabla}\bar{b}$ and $\boldsymbol{n} = |\nabla\bar{b}|^{-1}\nabla\bar{b}$ denote the unit vectors along and across the $\bar{b}$-contours, respectively.

The TEM eddy flux decomposition can be found in Andrews and McIntyre (1978) and is used for instance by Nakamura (2001), Greatbatch (2001) and Olbers and Visbeck (2005). In the TEM, B acts as a streamfunction for the eddy-induced tracer advection velocity $\boldsymbol{u}_{eddy} = -\,\underset{\neg}{\nabla}B$. The sum $\boldsymbol{u}_{eddy} + \bar{\boldsymbol{u}}$ is sometimes called the "residual velocity". It is the residual velocity which advects the mean tracer $\bar{b}$ and, in addition, an eddy-induced diffusion term with diffusivity K shows up in the mean tracer budget

$$\bar{b}_t + (\bar{\boldsymbol{u}} - \;\underset{\neg}{\nabla}B)\cdot\nabla\bar{b} \;\; = \;\; \bar{Q} + \nabla\cdot K\nabla\bar{b} \tag{10}$$

The eddy-induced diffusivity K vanishes only for $\boldsymbol{F} \cdot \nabla \bar{b} = 0$, i. e. if the eddy fluxes have locally no cross-isopycnal component. In the limit $|\bar{b}_z| >> |\bar{b}_y|$ i. e. for a strongly stratified situation, the eddy streamfunction becomes $B = -\overline{v'b'}/\bar{b}_z$ (Andrews and McIntyre, 1976), while for $|\bar{b}_y| >> |\bar{b}_z|$ e. g. in the oceanic mixed layer, the eddy streamfunction becomes $B = \overline{w'b'}/\bar{b}_y$ (Held and Schneider, 1999). However, it should be stressed that the flux decompositions by Andrews and McIntyre (1976), $B = -\overline{v'b'}/\bar{b}_z$, and Held and Schneider (1999), $B = \overline{w'b'}/\bar{b}_y$, are both choices for the streamfunction B in their own right and shouldn't be viewed as approximations to the TEM-G.

Fig. 2 (a) shows the (residual) streamfunction for the total flow, $(\bar{\boldsymbol{u}} - \underline{\nabla} B)$, in experiment CHANNEL-3. The value for the residual streamfunction ranges from 0 to $-30\, m^2/s$. Note that this streamfunction is given for the zonally averaged flow and that a value of $30\, m^2/s$ corresponds to about $30\, Sv$ per 10^o longitude volume transport in this model setup. The streamfunction of the Eulerian mean flow in CHANNEL-3 ($-\underline{\nabla} B_m = \bar{\boldsymbol{u}}$, not shown explicitly) in the interior of the channel is much smaller (only up to $3\, m^2/s$) than the eddy streamfunction B, only in the restoring zones the mean streamfunction reaches values comparable to the eddy streamfunction. Thus, the meridional overturning in the interior of the channel is dominantly eddy-driven in this setup. Note that in addition to the meridional overturning, there is a strong zonal transport of about $400\, Sv$ (not shown).

The residual streamfunction (Fig. 2 a) shows rather strong cross-isopycnal flow in the interior of the channel. Consequently, the diffusivity K in the TEM is rather large: Fig. 2 (d) shows the diagnosed eddy-induced diffusivity (K) in the TEM for experiment CHANNEL-3, with values of more than $100\, cm^2/s$ at maximum in the interior of the channel. Note that K inside the restoring zones is greatly exceeding $100\, cm^2/s$ and that K in the TEM becomes negative in some interior regions.

Going to higher resolution (and therefore less spurious diabatic forcing Q) changes the results only slightly. Fig. 3 a) and Fig. 4 a) show the residual streamfunction in the TEM in experiments CHANNEL-6 and CHANNEL-12 respectively and Fig. 3 d) and Fig. 4 d) the respective eddy-induced diffusivities K in the TEM. There is still strong cross-isopycnal flow in

the residual streamfunctions and considerable large values of K in the higher resolution model configurations. Note that the regions in which K is negative remain more or less the same in all experiments and, if anything, show evidence of expanding into the interior.

In the TEM, the eddy-induced diffusivity K vanishes only if the eddy tracer fluxes are directed entirely along isopycnals. It is however unclear if the fluxes will locally satisfy $\boldsymbol{F}\cdot\nabla\bar{b} = 0$ in the adiabatic limit when $Q = 0$, i. e. it is unclear if statement i) is satisfied by the TEM. Using the TEM flux decomposition in the integral constraint Eq. (5)

$$\int_{s_0}^{s_1} \overline{\boldsymbol{u}'b'}\cdot\boldsymbol{n}\,ds = -\int_{s_0}^{s_1} K|\nabla\bar{b}|ds = \int_A dA(\bar{Q} - \frac{\partial}{\partial t}\bar{b}) \tag{11}$$

it becomes clear that only a "mean" K in the TEM averaged along a mean isopycnal (and weighted by $|\nabla\bar{b}|$) becomes zero in the adiabatic and quasi-steady case, while this cannot be shown for the local value of K. In our numerical experiments, which are in quasi-steady state, K in the TEM is large and fluctuates around zero on a mean isopycnal and this behaviour does not decrease going to less diabatic flow regimes in higher resolution. Thus, on the basis of our numerical experiments in which we have done our best to come close to the adiabatic case, we conclude that the TEM is not in accordance with statement i).

4 Rotational eddy fluxes

4.1 Motivation

We demonstrate in this section that large rotational eddy fluxes are the reason for the large K of fluctuating sign along a mean isopycnal in the classical TEM formalism and the related inconsistency of the TEM with statement i). Such rotational eddy fluxes do not effect the mean tracer budget Eq. (3) but do effect the definitions for B and K. Consider the flux decomposition

$$\boldsymbol{F} \;=\; \underset{\neg}{\nabla}\theta + B\,\underset{\neg}{\nabla}\bar{b} - K\nabla\bar{b} \tag{12}$$

where $\underset{\neg}{\nabla}\theta$ serves as a rotational gauge flux which drops out from the divergence of $\boldsymbol{F}$. Note that Eq. (12) is not a classical Helmholtz decomposition, since we are not insisting that all of

the rotational part of the eddy tracer flux $\boldsymbol{F}$ is carried by $\underset{\neg}{\nabla}\theta$. The remainder $\boldsymbol{F} - \underset{\neg}{\nabla}\theta$ might still show some rotational part. The eddy streamfunction B and diapycnal diffusivity K are now given by

$$B = |\nabla\bar{b}|^{-2}(\boldsymbol{F} - \underset{\neg}{\nabla}\theta)\cdot\ \underset{\neg}{\nabla}\bar{b} = \quad |\nabla\bar{b}|^{-1}(F_{||} - \frac{\partial}{\partial n}\theta) \tag{13}$$

$$K = -|\nabla\bar{b}|^{-2}(\boldsymbol{F} - \underset{\neg}{\nabla}\theta)\cdot\nabla\bar{b} = -|\nabla\bar{b}|^{-1}(F_{\perp} + \frac{\partial}{\partial s}\theta) \tag{14}$$

introducing the along, $\frac{\partial}{\partial s}() = \boldsymbol{s}\cdot\nabla()$, and cross, $\frac{\partial}{\partial n}() = \boldsymbol{n}\cdot\nabla()$, isopycnal derivatives.

We will discuss here a choice for θ which was originally proposed by Gille and Davis (1999) (their Ψ_{opt}) and which corresponds to the effective eddy diffusivity concept of Nakamura (2001). This modification of the classical TEM for diabatic flow is called hereafter the TEM-D. The rotational gauge potential θ in the TEM-D follows from a minimisation of the eddy-induced diffusivity as outlined in Appendix A. The difference to the classical TEM is that it is not the local diapycnal eddy flux, $F_{\perp}$, which determines K but the averaged flux along an isopycnal, $\int_{s_0}^{s_1} F_{\perp}(s,n)ds$. As seen in the integral budget Eq. (5) this integrated flux goes to zero for the adiabatic and quasi-steady case, thus the TEM-D is in agreement with statement i), while the classical TEM is not.

4.2 The adiabatic TEM

We begin by discussing the simple choice

$$\theta = -\int_{s_0}^{s} F_{\perp}ds' \tag{15}$$

for which we get obviously $K = 0$ in Eq. (14). In the quasi-steady case, $\bar{b}_t = 0$, the residual flow in the mean tracer budget is then purely along contours of $\bar{b}$, and for $Q = 0$, the choice would be in agreement with statement i) from section 1. We call this flux decomposition the adiabatic TEM, thus the TEM-A.

Although in principle mathematically valid, it is shown in Appendix B that applying the TEM-A to diabatic flows, i. e. with $Q \neq 0$, the integrated cross-isopycnal eddy flux is redirected as a rotational flux through the boundary of the channel, a rather unphysical result.

Only in quasi-steady, purely adiabatic conditions, is the integrated cross-isopycnal eddy flux zero (Eq. (5)) and the TEM-A an acceptable flux decomposition. In fact, the TEM-A nicely demonstrates that setting $K = 0$ in quasi-steady flows is physically justified only for the (hypothetical) adiabatic case, i. e. if $Q = 0$.

Clearly, in reality there is always diabatic forcing present and the numerical experiments discussed here certainly contain diabatic forcing. Therefore, the TEM-A does not appear to be a reasonable eddy flux interpretation for our application. However, the TEM-A remains useful as a diagnostic tool, to deduce the mean diabatic forcing $\bar{Q}$ in the numerical experiments. Note that estimating the "real" diabatic forcing $\bar{Q}$ in numerical models is rather difficult (Griffies et al., 2000; Eden and Oschlies, 2006), since there are no numerical advection schemes (even without any implicit diffusion, such as the classical "leapfrog"-scheme) which show the same properties as analytical advection, with the consequence that errors in the schemes have to be interpreted as diabatic forcing.

Applying the TEM-A in the quasi-steady, diabatic case yields

$$(\bar{\boldsymbol{u}} - \underline{\nabla} B) \cdot \nabla \bar{b} \;=\; \bar{Q} \tag{16}$$

i. e. only a nonzero $\bar{Q}$ can force cross-isopycnal residual flow, a feature of the TEM-A we now exploit for diagnosing the numerical experiments. Our aim is to compare $\bar{Q}$ with the eddy-induced mixing $\nabla \cdot K \nabla \bar{b}$ in the classical TEM case. Fig. 2 (b) shows the (residual) streamfunction for the total (meridional) flow $(\bar{\boldsymbol{u}} - \underline{\nabla} B)$ for TEM-A in experiment CHANNEL-3. In contrast to the classical TEM (Fig. 2 a), the residual flow of the TEM-A in the interior of the channel is more or less aligned along isopycnals with very little flow across isopycnals. Only inside the restoring zones does the residual streamfunction in the TEM-A show large cross-isopycnal flow, while the eddy-induced diffusivity K in the TEM-A (Fig. 2 e) fluctuates around zero diapycnal diffusivity, as expected by construction[6].

[6] Inside the restoring zones near the side walls of the channel, however, larger residuals of K in TEM-A show up for numerical reasons. Note that this artifact vanishes going to higher resolution, as in experiment CHANNEL-6 and CHANNEL-12, discussed below. Note that for the TEM-D (see below) the same artifact shows up in CHANNEL-3 and vanishes as well in CHANNEL-6 and CHANNEL-12.

In the TEM-A any cross-isopycnal (quasi-steady) flow is entirely driven by $\bar{Q}$. Therefore, we can conclude that the term $\nabla \cdot K \nabla \bar{b}$ in the TEM drives the strong cross-isopycnal residual flow in the interior of the channel evident in Figures 2 (a), 3 (a) and 4 (a). K in the classical TEM must be therefore much larger than an equivalent (mean) diapycnal diffusivity implied by $\bar{Q}$. Going to higher resolutions in CHANNEL-6 and CHANNEL-12, the picture hardly changes, i. e. the residual streamfunction is more or less aligned along mean isopycnals in the interior of the channel indicating that $\bar{Q}$ does not change much going to higher resolution.

4.3 The diabatic TEM

Now we return to the TEM-D eddy flux interpretation, originally proposed by Gille and Davis (1999) and which corresponds to the effective diffusivity concept of Nakamura (2001). Fig. 2 (c) shows the (residual) streamfunction for the total (meridional) flow ($\bar{\boldsymbol{u}} - \underset{\neg}{\nabla} B$) in TEM-D in experiment CHANNEL-3. The cross-isopycnal residual flow ranges between the strong cross-isopycnal flow in the classical TEM (Fig. 2 a) and the almost vanishing cross-isopycnal flow in the TEM-A (Fig. 2 b). Fig. 2 (f) shows the diagnosed eddy-induced diapycnal diffusivity K in the TEM-D for experiment CHANNEL-3. It ranges in between the extreme cases of the TEM and the TEM-A, as expected from the cross-isopycnal flow of the residual streamfunctions. Note that while K in the TEM becomes negative in some regions, this is not the case for the TEM-D. Since $|\nabla \bar{b}|$ does not vary much in our numerical experiments, K in the TEM-D shows almost no structure along a mean isopycnal. These uniform values of K reduce from about $100\,cm^2/s$ in CHANNEL-3 to about $50\,cm^2/s$ in CHANNEL-6 and about $20\,cm^2/s$ in CHANNEL-12. In all experiments, K in the TEM-D is essentially an average over the very large K's of the TEM inside the restoring zone near the side walls of the channel and the lower values in the interior.

There are strong rotational fluxes in the interior in all experiments (not shown). Note that in the TEM-D, the vertical rotational fluxes ($-\frac{\partial}{\partial y}\theta$) are of the same magnitude as the advective fluxes ($-B\frac{\partial}{\partial y}\bar{b}$) and the diffusive fluxes ($-K\frac{\partial}{\partial z}\bar{b}$) in all experiments and that the meridional rotational fluxes ($\frac{\partial}{\partial z}\theta$) are of the same magnitude as the advective fluxes ($B\frac{\partial}{\partial z}\bar{b}$) while the merid-

ional diffusive fluxes are orders of magnitude smaller. This demonstrates again the importance of the rotational fluxes in setting the shape and magnitudes of the eddy streamfunction B and the diffusivity K. Note also that the interior rotational fluxes become stronger in magnitude going to higher resolution, rather than getting smaller.

The TEM-D involves a nonlocal definition of the rotational gauge potential θ, which leads to an eddy-induced diffusivity which contains information throughout the channel about the strong diabatic forcing in the restoring zones near the northern and southern boundaries, even in regions in the interior which might be completely adiabatic. This is somehow an unsatisfactory result, also mentioned previously by Nurser and Lee (2004), and therefore we conclude that TEM-D is also an unsatisfactory eddy flux interpretation. In the next section, we will formulate another flux decomposition, which gives a more local definition of θ and the eddy-induced diffusivity in turn.

5 The Temporal Residual Mean

Adding a rotational non-divergent part to the eddy tracer flux $\boldsymbol{F}$ does not effect the mean tracer budget. However, it does effect the eddy variance equation, offering an opportunity to interpret this part of the flux. This fact was used by McDougall and McIntosh (1996) to develop the Temporal Residual Mean (TRM-I hereafter) extension to the TEM theory and later the TRM-II version (McDougall and McIntosh, 2001). We discuss here the more general and — in this context — simpler derivation, similar to what can be found in Greatbatch (2001) and Medvedev and Greatbatch (2004), and compare it with the above presented flux decompositions.

The eddy tracer fluxes are again expressed as in Eq. (12) where $\underset{\neg}{\nabla}\theta$ serves as a gauge flux which drops out when taking the divergence of $\boldsymbol{F}$ and so does not contribute to the mean tracer budget. Motivation for choosing a non-zero rotational potential θ comes from the budget of tracer variance ($\phi_2 = b'^2/2$), given by

$$(\overline{\phi_2})_t + \nabla \cdot \overline{\boldsymbol{u}\phi_2} \;=\; \overline{b'Q'} - \boldsymbol{F} \cdot \nabla \bar{b} \tag{17}$$

Using the flux decomposition Eq. (12) for $\boldsymbol{F}$ in the variance budget yields

$$(\overline{\phi_2})_t + \nabla \cdot \overline{\boldsymbol{u}\phi_2} \;=\; \overline{b'Q'} - \underset{\neg}{\nabla}\theta \cdot \nabla\bar{b} + K|\nabla\bar{b}|^2 \tag{18}$$

We now decompose the total (i. e. mean plus eddy) flux of eddy tracer variance into components along and across contours of $\bar{b}$ plus a rotational part, as we did before for the eddy tracer flux $\boldsymbol{F}$,

$$\overline{\boldsymbol{u}\phi_2} = \underset{\neg}{\nabla}\theta_2 + B_2 \underset{\neg}{\nabla}\bar{b} - K_2\nabla\bar{b} \tag{19}$$

where B_2 and K_2 are given by

$$B_2|\nabla\bar{b}| \;=\; \overline{\boldsymbol{u}\phi_2} \cdot \boldsymbol{s} - \frac{\partial}{\partial n}\theta_2 \tag{20}$$

$$K_2|\nabla\bar{b}| \;=\; -\overline{\boldsymbol{u}\phi_2} \cdot \boldsymbol{n} - \frac{\partial}{\partial s}\theta_2 \tag{21}$$

As before, $\mathbf{s}$ and $\mathbf{n}$ denote unit vectors along and perpendicular to the $\bar{b}$-contours, and $\frac{\partial}{\partial s}() = \boldsymbol{s} \cdot \nabla()$ and $\frac{\partial}{\partial n}() = \boldsymbol{n} \cdot \nabla()$ denote along and across isopycnal derivatives, respectively.

This yields the following set of equations

$$\bar{b}_t + (\bar{\boldsymbol{u}} - \underset{\neg}{\nabla}B) \cdot \nabla\bar{b} \;=\; \bar{Q} + \nabla \cdot K\nabla\bar{b} \tag{22}$$

$$(\overline{\phi_2})_t + \underset{\neg}{\nabla}(\theta - B_2) \cdot \nabla\bar{b} \;=\; \overline{b'Q'} + K|\nabla\bar{b}|^2 + \nabla \cdot K_2\nabla\bar{b} \tag{23}$$

As before we utilise the gauge freedom, now for θ and θ_2, to rephrase the mean tracer budget Eq. (22) and the variance budget Eq. (23). It is clear from Eq. (23) that it is natural to choose

$$\theta = B_2 \tag{24}$$

such that the rotational gauge potential is related to the along-isopycnal flux of variance by Eq. (20). Note that this choice follows the ideas of Marshall and Shutts (1981); McDougall and McIntosh (1996) and Medvedev and Greatbatch (2004). Second, we have to specify the rotational eddy variance flux given by $\underset{\neg}{\nabla}\theta_2$.

Medvedev and Greatbatch (2004), in their version of the TRM, put θ_2 to zero (a feature also of McDougall and McIntosh (1996), to whose approach Medvedev and Greatbatch (2004)

is closely related; see below). It is shown below that setting θ_2 to zero is inconsistent with statement i) for similar reasons as applied to the classical TEM discussed earlier. Analogous to the discussion of the TEM-A and the TEM-D, it is possible to define analogous TRM versions, namely an "adiabatic" TRM (TRM-A hereafter) and a "diabatic" TRM (TRM-D hereafter). However, this route is not discussed in detail here, we just note the following features of such flux decompositions:

For TRM-A, all the cross-isopycnal flux of variance is absorbed into a rotational flux, and $K_2 = 0$, while for the TRM-D version we would get again an "isopycnally averaged" version of K_2, i. e. $K_2 = -|\nabla\bar{b}|^{-1}G_2(n)$ with $G_2 = (s_1 - s_0)^{-1}\int_{s_0}^{s_1}\overline{\boldsymbol{u}\phi_2}\cdot\boldsymbol{n}\,ds$. For the TRM-A, in general, for diabatic flows, there are rotational fluxes of variance across the side walls, given by G_2, but which are zero in the TRM-D. Again analogous to the discussion about the TEM-A/D, it is possible to show that this cross-boundary rotational flux of variance will go to zero in the quasi-steady and adiabatic limit, by considering the integral budgets of eddy and mean tracer variance above a mean isopycnal. Furthermore, in the quasi-steady and adiabatic limit, the TRM-A and TRM-D are identical. In fact, in this limit $K_2 = 0$, and $K = 0$, and all four flux decompositions (the TRM-A, TRM-D, TEM-A and TEM-D) collapse into the same, identical decomposition..

On the other hand, it is also easy to see that setting $\theta_2 = 0$, as in the TRM-M version of Medvedev and Greatbatch (2004), K_2 will be given by the divergence of the cross-isopycnal flux of variance, which is not guaranteed to be locally zero in the quasi-steady and adiabatic limit. Thus, from the variance budget Eq. (23) it follows that for the TRM-M, K will also not necessarily be zero in the quasi-steady and adiabatic limit, i. e. the TRM-M is inconsistent with statement i). It should also be noted that the difference between TRM-M and TRM-I (McDougall and McIntosh, 1996) is given by assuming in the TRM-I that $\overline{\boldsymbol{u}'\phi_2} \approx 0$.

It is possible to extend the ideas of Greatbatch (2001) to the full hierarchy of moments which yields a generalised form of the TRM along the ideas of Marshall and Shutts (1981); McDougall and McIntosh (1996) and Greatbatch (2001) and which avoids any non-local definition of the rotational gauge potential θ. This eddy flux decomposition is called the TRM-G (the

Generalised Temporal Residual Mean) hereafter.

The hierarchy of tracer moments is given by

$$(\overline{\phi_{n+1}})_t + \nabla \cdot \overline{\boldsymbol{u}\phi_{n+1}} + n\overline{\phi_n \boldsymbol{u}} \cdot \nabla \bar{b} = n\overline{\phi_n Q} - n\bar{\phi}_n \bar{b}_t \tag{25}$$

with $\phi_n = \frac{b'^n}{n}$. Note that the advective terms and the dissipation term in Eq. (25) contain the full velocity $\boldsymbol{u}$ and the full forcing Q. As before, for the eddy tracer flux $\boldsymbol{F}$ (Eq. (12)) and the eddy tracer variance flux $\overline{\boldsymbol{u}\phi_2}$ (Eq. (19)), a similar flux decomposition is also applied to the fluxes of higher order variances

$$\overline{\boldsymbol{u}\phi_n} = \underset{\neg}{\nabla}\theta_n + B_n \underset{\neg}{\nabla}\bar{b} - K_n \nabla \bar{b} \tag{26}$$

which yields the following set of equations

$$\bar{b}_t + (\bar{\boldsymbol{u}} - \underset{\neg}{\nabla} B) \cdot \nabla \bar{b} = \bar{Q} + \nabla \cdot K \nabla \bar{b} \tag{27}$$

$$(\overline{\phi_2})_t + \underset{\neg}{\nabla}(\theta - B_2) \cdot \nabla \bar{b} = \overline{b'Q'} + K|\nabla \bar{b}|^2 + \nabla \cdot K_2 \nabla \bar{b} \tag{28}$$

$$(\overline{\phi_{n+1}})_t + \underset{\neg}{\nabla}(n\theta_n - B_{n+1}) \cdot \nabla \bar{b} = n\overline{\phi_n Q} - n\bar{\phi}_n \bar{b}_t + \ + nK_n|\nabla \bar{b}|^2 + \nabla \cdot K_{n+1} \nabla \bar{b} \tag{29}$$

Note that Eq. (29) gives the budget for the higher order moments $\overline{\phi_{n+1}}$ using the flux decomposition Eq. (26), and the other two budgets are simply a repetition from above. We extend the ideas of Greatbatch (2001) and set $\theta = B_2$ and $n\theta_n = B_{n+1}$ in the full hierarchy of equations. Introducing the along-isopycnal fluxes $J_n = \overline{\boldsymbol{u}\phi_n} \cdot \boldsymbol{s}$, and using the setting

$$n\theta_n = B_{n+1} = |\nabla \bar{b}|^{-1}(J_{n+1} - \frac{\partial}{\partial n}\theta_{n+1}) \tag{30}$$

iteratively in the equations Eq. (13) and Eq. (14) for the eddy streamfunction B and the eddy-induced diffusivity K, respectively, yields the following set of equations for the B, K and the rotational gauge potential θ in the TRM-G

$$B|\nabla \bar{b}| = F_{\parallel} - \frac{\partial}{\partial m}J_2 + \frac{1}{2}(\frac{\partial}{\partial m})^2 J_3 - \frac{1}{3!}(\frac{\partial}{\partial m})^3 J_4 + ... \tag{31}$$

$$K|\nabla \bar{b}| = -F_{\perp} - \frac{\partial}{\partial s}\theta \tag{32}$$

$$\theta|\nabla \bar{b}| = J_2 - \frac{1}{2}\frac{\partial}{\partial m}J_3 + \frac{1}{3!}(\frac{\partial}{\partial m})^2 J_4 - ... \tag{33}$$

introducing the operator $\frac{\partial}{\partial m}() = \frac{\partial}{\partial n}|\nabla\bar{b}|^{-1}()$. Using the variance budgets Eq. (29) we can express the eddy-induced diapycnal diffusivity in quasi-steady (but diabatic) conditions also as

$$K|\nabla\bar{b}|^2 = -\overline{b'Q'} + \mathcal{D}(\overline{\phi_2 Q}) - \frac{1}{2}\mathcal{D}^2(\overline{\phi_3 Q}) + \frac{1}{3!}\mathcal{D}^3(\overline{\phi_4 Q}) - \frac{1}{4!}\mathcal{D}^4(\overline{\phi_4 Q}) + ... \tag{34}$$

or for the adiabatic (but unsteady) regime as

$$K|\nabla\bar{b}|^2 \;\; = \;\; (\overline{\phi_2})_t - \frac{1}{2}\mathcal{D}(\overline{\phi_3})_t + \frac{1}{3!}\mathcal{D}^2(\overline{\phi_4})_t - \mathcal{D}(\bar{\phi}_2\bar{b}_t) + \frac{1}{2}\mathcal{D}^2(\bar{\phi}_3\bar{b}_t) - \frac{1}{3!}\mathcal{D}^3(\bar{\phi}_4\bar{b}_t) + ... \tag{35}$$

introducing the operator $\mathcal{D}() = \nabla\cdot\nabla\bar{b}|\nabla\bar{b}|^{-2}()$. Note that for the general case (unsteady and diabatic) Eq. (34) and Eq. (35) will simply add. The TRM-G for the three-dimensional case and temporal averaging is outlined in Appendix C.

We see that K in the TRM-G will be zero in the adiabatic and quasi-steady regime, and thus the TRM-G is in accordance with statement i). As a result, we have constructed a fully consistent flux decomposition based on the ideas of Marshall and Shutts (1981); McDougall and McIntosh (1996) and Greatbatch (2001), which can be evaluated for any stratification and to any order and which gives a locally defined eddy-induced diffusivity and eddy streamfunction. This is the main result of this paper.

Note that the TEM-A, TEM-D and TRM-G collapse into a single flux decomposition in the adiabatic case. It is also easy to see that the definition for the streamfunction B in the TRM-G is identical to the classical TEM in the first term of the series in Eq. (31), and to the TRM-M in the first and second term. The same holds for K in Eq. (32) after substituting for θ from Eq. (32).

Fig. 5 shows the eddy-induced diffusivity K in the TRM-G, calculated in CHANNEL-6 with increasing orders in perturbation amplitude. For Fig. 5 a) K is evaluated to the first term in the series, i. e. $K|\nabla\bar{b}| = -F_\perp$ which is the same as K in the TEM; Fig. 5 b) uses K to the second term, which is the same as K in the TRM-M; c) is to the third term and d) to 4th term. Note that the TRM-I by McDougall and McIntosh (1996) (not shown) is very similar to the classical TEM in our setup. There is a large decrease in magnitude of K in the interior of the

channel going from the first term (a, equivalent to the TEM) to the second term (b, equivalent to the TRM-M). However, there are still regions of negative K in the TRM-M. These regions are further reduced and are subsequently vanish including also higher order terms in the TRM-G. On the other hand, the corrections to K are decreasing in higher orders, showing the rapid convergence of the TRM-G in our experimental setup.

Note that the diffusivity K evaluated to the second term (Fig. 5 b) appears to be a reasonable approximation to the full form (excluding the regions of negative K). Since this K is almost identical to that given by the first term in (33), i.e. $K = -(\nabla\bar{b})^{-2}\overline{Q'b'}$, we conclude that the first term in (33) provides a reasonable expression for a local definition of K to be used in a parameterisation (at least in our experiments). Note also that there are still very large values of K in the TRM-G inside the restoring zones, much larger than the "mean" value of K in the TEM-D. On the other hand, interior values of K are small in the TRM-G in the range of about $20\,cm^2/s$, i. e. much smaller than the corresponding averaged values of K in the TEM-D. Fig. 6 shows the residual streamfunction in the TRM-G, calculated in CHANNEL-6 again with increasing orders in perturbation amplitude.

6 Summary and discussion

It was our aim, formulated in statement i) in Section 1, to represent the effect of eddy fluxes locally as a purely isopycnal flux in the adiabatic and quasi-steady case. It was shown that this is not guaranteed to be the case for the classical TEM formalism by Andrews and McIntyre (1978) and, as shown in numerical experiments, the implied eddy-induced diapycnal diffusion can become large with large changes of sign on a mean isopycnal. The experiments also show that this behaviour does not reduce going to higher resolution and thus less diabatic forcing. We have identified rotational eddy tracer fluxes as being responsible for this behaviour.

Setting all diffusive eddy-effects in the mean tracer budget to zero by introducing a non-locally defined rotational flux in the eddy tracer fluxes yields only for the (hypothetical) case of adiabatic flow a reasonable eddy flux interpretation (thus called here the TEM-A). Applying

the TEM-A to diabatic flows yields an unphysical cross-boundary rotational eddy tracer flux, demonstrating that implying zero eddy-induced diffusivity is physically unreasonable for diabatic flow regimes. On the other hand, the TEM-A proves to be useful as a diagnostic of the mean diabatic forcing in the numerical experiments, which is otherwise hard to estimate.

A consistent extension of the TEM-A to diabatic regimes is called the TEM-D which was originally proposed by Gille and Davis (1999) and which corresponds to the effective diffusivity concept of Nakamura (2001). Here, a minimal eddy-induced diapycnal diffusion shows up again in the mean tracer budget, which vanishes only in the adiabatic regime. This result points again toward the physical relevance of eddy-induced diapycnal mixing for diabatic flows. The TEM-D collapses to the TEM-A in the adiabatic, quasi-steady limit, thus the TEM-D is in agreement with statement i).

However, since the eddy-induced diffusivity in the TEM-D is given by an average of the eddy tracer flux across a mean isopycnal, it can include information from strong non-local diabatic forcing even in completely adiabatic regions. In our numerical channel experiments, the strong forcing inside the restoring zones gives rise to large diffusivities in the interior (note that they are positive definite in all experiments). We conclude that this feature of the TEM-D (and the effective diffusivity by Nakamura (2001)) is a rather unsatisfactory result. Furthermore, such a non-local definition of the diffusivity and streamfunction might be difficult to parameterise.

The TEM versions consider first order moments. In contrast, the TRM originally proposed by McDougall and McIntosh (1996) consider the eddy tracer variance equation to find gauge fluxes for the eddy tracer flux. We have generalised the concept and found the TRM-G which collapses to the TEM-A/D in the adiabatic limit, but avoids any integral definitions of the rotational gauge fluxes. In contrast, the eddy streamfunction and the eddy-induced diffusivity in the TRM-G are given by an infinite series involving fluxes of eddy tracer moments, since the flux decomposition was derived from an infinite hierarchy of budgets for tracer moments. Truncating the infinite series for the eddy-induced streamfunction and diffusivity in the TRM-G after the first term gives the classical TEM and truncating after the second term gives the TRM-M by Medvedev and Greatbatch (2004) for which the special case $|b_z| >> |b_y|$ and

$\overline{v'\phi_2} \approx 0$ leads to the TRM-I by McDougall and McIntosh (1996).

While the TRM-M and the TRM-I are not necessarily satisfying statement i), for similar reasons as before for the classical TEM version, the new concept, the TRM-G, is in agreement with statement i) and can be evaluated for any stratification and to any order. It should also be noted that all arguments here carry over in a straightforward manner to three dimensions and temporal averaging, and can also be applied to isopycnal averaging to take account of rotational fluxes, e. g. on an isopycnal surface.

We have formulated in statement i), that there is no (local) diapycnal mixing by eddies unless there is some other (local) small-scale diapycnal forcing or mixing process at work. However, if there is such a small-scale diapycnal mixing, the TRM-G quantifies to what extent mesoscale eddy activity is able to locally enhance (or reduce) this mixing, i. e. how the large-scale mean quantities are affected by the small scale mixing processes. The TRM-G relates eddy-induced diapycnal diffusivity locally to

- either growth or decay of mesoscale density variance and higher order moments and/or
- covariances between the small-scale forcing or mixing and density fluctuations.

The eddy-induced mixing effect is rather strong in our numerical model and might be overestimated, but we think, that the traditional view that eddies are mixing completely adiabatically has to be revised, as proposed by Tandon and Garrett (1996) and recently by Radko and Marshall (2004). We note too, that our formula for the eddy-induced diffusivity, Eq. (33), suggests that the diffusivity can be expected to large where the diapycnal forcing, Q, and its associated fluctuations, Q', are large, suggesting that the diffusivity is large in the surface mixed layer, but relatively small in the much more adiabatic ocean interior, an issue we explore elsewhere.

Since it is possible to extend the TRM-G theory to any tracer, the formalism thus relates, for the general case, a three-dimensional turbulent diffusivity to *local* changes and/or dissipation of tracer variance. Note that such a local relation in the tracer variance budget is also assumed and extensively used in homogeneous turbulence theory and in several turbulence closures. Using

the TRM-G, it is possible to "localise" the variance budget also for the spatially inhomogeneous case.

Acknowledgments

We want to thank J. Willebrand, A. Oschlies, A. Medvedev and S. Danilov for stimulating discussions. We also thank George Nurser, an anonymous reviewer and the editor for helpful comments. The model integrations have been performed on a NEC-SX5 at the computing centre at the University Kiel, Germany. RJG also thanks NSERC and CFCAS for financial support through an NSERC Research Grant and the Canadian CLIVAR Research Network.

Appendix A

Since $\underset{\neg}{\nabla}\theta$ makes no contribution to the mean tracer budget, there is flexibility in the choice of θ, a flexibility which is exploited here. We ask for a θ in the flux decomposition in Eq. (12) that minimises (in some sense) $K\nabla\bar{b}$ which denotes the cross-isopycnal eddy flux, when specifying b as potential density. This leads to the following minimisation problem

$$\frac{1}{2}\int W(K\nabla\bar{b})^2 dydz = min \tag{36}$$

where $W(y,z)$ denotes a weighting function which is specified below. The corresponding Euler-Lagrange equation[7] is

$$\underset{\neg}{\nabla}\bar{b}\cdot\nabla\left[\frac{W}{|\nabla\bar{b}|^2}\left(\boldsymbol{F}\cdot\nabla\bar{b}+\nabla\theta\cdot\ \underset{\neg}{\nabla}\bar{b}\right)\right]=0 \tag{37}$$

which states that the term inside the brackets is constant along contours of $\bar{b}$. It is convenient to use again coordinates along (s) and perpendicular (n) to contours of $\bar{b}$ together with the along, $\frac{\partial}{\partial s}() = \boldsymbol{s}\cdot\nabla()$, and cross, $\frac{\partial}{\partial n}() = \boldsymbol{n}\cdot\nabla()$, isopycnal derivatives, so that the bracketed term in Eq. (37) becomes

$$F_\perp(s,n)+\frac{\partial\theta(s,n)}{\partial s}=G(n) \tag{38}$$

[7]Note that all results presented here carry over to three dimensions, including the solution of the Euler-Lagrange equation.

by specifying W as $W = |\nabla\bar{b}|$. We get as the optimal vector gauge potential

$$\theta(s,n) = \int_{s_0}^{s} (G(n) - F_\perp) ds' + H(n) \tag{39}$$

and for the eddy-induced diapycnal diffusivity, in turn,

$$K = -|\nabla\bar{b}|^{-1}(F_\perp + \frac{\partial\theta}{\partial s}) = -|\nabla\bar{b}|^{-1} G(n) \tag{40}$$

with arbitrary functions $G(n)$ and $H(n)$.

Setting the integration constant $G(n)$ in Eq. (40) to zero, we get zero eddy-induced diffusivity K as the minimal value and the TEM-A version, see above and Appendix B. To obtain no rotational eddy tracer flux through the boundaries in the diabatic case, we must insure that $\theta = const$ along the boundaries, i. e.

$$G(n) = (s_1 - s_0)^{-1} \int_{s_0}^{s_1} F_\perp(s,n) ds = F_{ave}(n) \tag{41}$$

For this choice there is an eddy-induced diffusivity given by the cross-isopycnal eddy fluxes averaged along an isopycnal. The difference to the classical TEM is that it is not the local cross-isopycnal eddy flux, $F_\perp$, which determines K but the averaged flux, $\int_{s_0}^{s_1} F_\perp(s,n) ds$. What is left in K is the minimal diapycnal flux which is needed to constrain the no-flow boundary condition for the rotational eddy flux. We call this flux decomposition the TEM-D. Note that the TEM-D was originally proposed by Gille and Davis (1999) and corresponds to the effective (eddy-induced) diffusivity concept by Nakamura (2001), recently used, for instance, by Marshall et al. (2006). In order to diagnose the TEM-D in the numerical experiments, we simply use $\theta = 0$ as boundary condition to solve Eq. (37) using the same procedure as for the TEM-A.

The TEM-D approaches the classical TEM in the following limit: If the eddy tracer flux is entirely along contours of $\bar{b}$, i. e. if $\boldsymbol{F} \cdot \nabla\bar{b} = 0$ everywhere, the rotational potential θ and in consequence the rotational eddy tracer flux is zero. For this case the eddy streamfunction and diffusivity (which is also zero) become the same as in the TEM. Approaching the adiabatic limit, $Q = 0$, the TEM-D becomes the TEM-A under general circumstances. Note that the classical TEM does not necessarily approach the TEM-A in this limit. Therefore, the TEM-D is in accordance with statement i) while the classical TEM disagrees with it.

Appendix B

Although mathematically valid in principle, applying the TEM-A to diabatic flows, i. e. with $Q \neq 0$, yields an inconsistency. This can be seen considering again the integral constraint Eq. (5) for diabatic flows, using the flux decomposition Eq. (12) with θ from Eq. (39) with $G = 0$

$$\theta|_{s_1} - \theta|_{s_0} = \int_{s_0}^{s_1} F_\perp ds = \int_A dA(\bar{Q} - \bar{b}_t) \tag{42}$$

This shows that starting the integration of θ at $s = s_0$ where the mean isopycnal intersects a lateral boundary of the channel, must yield a different value of θ at the other boundary at $s = s_1$, since the cross-isopycnal eddy flux does not integrate to zero for $Q \neq 0$ (and $\bar{b}_t \neq 0$). Since θ acts as a streamfunction for a rotational eddy flux, there must be a rotational eddy flux through the lateral boundary at s_1 given by $\int_A dA(\bar{Q} - \bar{b}_t)$. Thus setting $K = 0$ by the choice of θ in the TEM-A for diabatic flows redirects the integrated cross-isopycnal eddy flux as a rotational flux through the boundary, a rather unphysical result.

To diagnose the TEM-A in the numerical experiments, θ is calculated by interpolating $\boldsymbol{F}(y, \bar{b}(y, z)) \cdot \nabla\bar{b}/|\nabla\bar{b}|$ to an equidistant grid in the new coordinate $\bar{b}$ and integrating this quantity along lines of constant $\bar{b}$, starting at the southern end of the channel, where we put $\theta = 0$. In this way, we obtain $\theta(y, \bar{b}) = -\int_{s_0}^{s} F_\perp ds'$ and then interpolate θ back to z as vertical coordinate. This θ serves then as the boundary condition to solve the Euler-Lagrange Eq. (37). Note that the last step is formally not needed, but smoothes the solution for θ.

Appendix C

The extension of the above discussion of the TRM-G to the three-dimensional case and temporal averaging is straightforward. Its consequences are briefly outlined here. In the mean tracer budget Eq. (3) and the hierarchy of tracer moments Eq. (25) the two-dimensional operator ∇ is replaced by its three-dimensional equivalent ∇_3. The decomposition of the (three-dimensional)

eddy tracer flux $\boldsymbol{F}$ (Eq. (12)), the eddy tracer variance flux $\overline{\boldsymbol{u}\phi_2}$ (Eq. (19)), and the fluxes of higher order variances (Eq. (26)) become

$$\overline{\boldsymbol{u}\phi_n} = \nabla_3 \times \boldsymbol{\theta}_n + \boldsymbol{B}_n \times \nabla_3 \bar{b} - K_n \nabla_3 \bar{b} \tag{43}$$

where $\boldsymbol{B}_n$ and $\boldsymbol{\theta}_n$ denote three-dimensional vectors. Note that $\boldsymbol{B}_1$ becomes a vector streamfunction for the three-dimensional eddy-driven flow $\boldsymbol{u}^* = \nabla_3 \times \boldsymbol{B}$, while the eddy-induced diffusivity K_1 remains to be a scalar.

The along-isopycnal fluxes of tracer moments become in three-dimensions $\boldsymbol{J}_n = \boldsymbol{n}_3 \times \overline{\boldsymbol{u}\phi_n}$ with $\boldsymbol{n}_3 = |\nabla_3|^{-1} \nabla_3 \bar{b}$. The setting Eq. (30) becomes

$$n\boldsymbol{\theta}_n = \boldsymbol{B}_{n+1} = |\nabla_3 \bar{b}|^{-1} (\boldsymbol{J}_{n+1} - \frac{\partial}{\partial n_3} \theta_{n+1}) \tag{44}$$

with $\frac{\partial}{\partial n_3}() = -\boldsymbol{n}_3 \times [\nabla_3 \times ()]$ and the expression for the eddy streamfunction $\boldsymbol{B}$, eddy-induced diffusivity K and vector gauge potential $\boldsymbol{\theta}$

$$\boldsymbol{B}|\nabla_3 \bar{b}| = \boldsymbol{J}_1 - \frac{\partial}{\partial m_3} \boldsymbol{J}_2 + \frac{1}{2}(\frac{\partial}{\partial m_3})^2 \boldsymbol{J}_3 - \frac{1}{3!}(\frac{\partial}{\partial m_3})^3 \boldsymbol{J}_4 + ... \tag{45}$$

$$K|\nabla_3 \bar{b}| = -\boldsymbol{F} \cdot \boldsymbol{n}_3 - \frac{\partial}{\partial s_3} \boldsymbol{\theta} \tag{46}$$

$$\boldsymbol{\theta}|\nabla_3 \bar{b}| = \boldsymbol{J}_2 - \frac{1}{2}\frac{\partial}{\partial m_3} \boldsymbol{J}_3 + \frac{1}{3!}(\frac{\partial}{\partial m_3})^2 \boldsymbol{J}_4 - ... \tag{47}$$

with $\frac{\partial}{\partial m_3}() = \frac{\partial}{\partial n_3} |\nabla_3 \bar{b}|^{-1}()$ and $\frac{\partial}{\partial s_3}() = \boldsymbol{n}_3 \cdot \nabla_3 \times ()$.

References

Andrews, D. G. and M. E. McIntyre, 1976: Planetary waves in horizontal and vertical shear: The generalized Eliassen-Palm relation and the zonal mean accelaration. *J. Atmos. Sci.*, **33**, 2031–2048.

Andrews, D. G. and M. E. McIntyre, 1978: Generalized Eliassen-Palm and Charney-Drazin theorems for waves on axisymmetric mean flows in compressible atmosphere. *J. Atmos. Sci.*, **35**, 175–185.

Eden, C. and A. Oschlies, 2006: Effective diffusivities in model of the North Atlantic. Part I: subtropical thermocline. *J. Phys. Oceanogr.*. Submitted.

Gille, S. T. and E. E. Davis, 1999: The influence of mesoscale eddies on coarsely resolved density: an examination of subgrid-scale parameterization. *J. Phys. Oceanogr.*, **29**, 1109–1123.

Greatbatch, R. J., 2001: A framework for mesoscale eddy parameterization based on density-weighted averaging at fixed height. *J. Phys. Oceanogr.*, **31**(9), 2797–2806.

Griffies, S. M., R. C. Pacanowski, and B. R. Hallberg, 2000: Spurious diapycnal mixing associated with advection in a z-coordinate ocean model. *Mon. Wea. Rev.*, **128**, 538–564.

Hasselmann, K., 1982: An ocean model for climate variability studies. *Prog. Oceanogr.*, **11**, 69–92.

Held, I. M. and T. Schneider, 1999: The surface branch of the zonally averaged mass transport circulation in the troposphere. *J. Atmos. Sci.*, **56**(11), 1688–1697.

Leonard, B. P., 1979: A stable and accurate convective modelling procedure based on quadratic upstream interpolation. *Computer Methods in Applied Mechanics and Engineering*, **19**, 59–98.

Marshall, J., E. Shuckburgh, H. Jones, and C. Hill, 2006: Estimates and implications of surface eddy diffusivity in the southern ocean derived from tracer transport. *J. Phys. Oceanogr.*. In press.

Marshall, J. and G. Shutts, 1981: A note on rotational and divergent eddy fluxes. *J. Phys. Oceanogr.*, **11**(12), 1677–1679.

McDougall, T. J., 1987: Neutral surfaces. *J. Phys. Oceanogr.*, **17**, 1950–1964.

McDougall, T. J. and P. C. McIntosh, 1996: The temporal-residual-mean velocity. Part I: Derivation and the scalar conservation equation. *J. Phys. Oceanogr.*, **26**, 2653–2665.

McDougall, T. J. and P. C. McIntosh, 2001: The temporal-residual-mean velocity. Part II: Isopycnal interpretation and the tracer and momentum equations. *J. Phys. Oceanogr.*, **31**(5), 1222–1246.

Medvedev, A. S. and R. J. Greatbatch, 2004: On advection and diffusion in the mesosphere and lower thermosphere: The role of rotational fluxes. *J. Geophys. Res.*, **109**(D07104, 10.1029/2003JD003931).

Nakamura, N., 2001: A new look at eddy diffusivity as a mixing diagnostic. *J. Atmos. Sci.*, **58**, 3695–3701.

Nurser, A. J. G. and M.-M. Lee, 2004: Isopycnal averaging at constant height: Part I: the formulation and a case study. *J. Phys. Oceanogr.*, **34**(12), 2721–2739.

Olbers, D. and M. Visbeck, 2005: A zonally averaged model of the meridional overturning in the Southern Ocean. *J. Phys. Oceanogr.*, **35**, 1190–1205.

Pacanowski, R. C., 1995: MOM 2 Documentation, User's Guide and Reference Manual. Technical report, GFDL Ocean Group, GFDL, Princeton, USA.

Radko, T. and J. Marshall, 2004: Eddy-induced diapycnal fluxes and their role in the maintenance of the thermocline. *J. Phys. Oceanogr.*, **34**, 372–383.

Tandon, A. and C. Garrett, 1996: On a recent parameterization of mesoscale eddies. *J. Phys. Oceanogr.*, **26**(3), 406–416.

Wüst, G., 1935: Schichtung und Zirkulation des Atlantischen Ozeans. Die Stratoshäre des Atlantischen Ozeans. *Wiss. Ergebn. Dt. Atlant. Exped. "Meteor" 1925–1927*, **6**, 109–288.

List of Figures

1 Instantaneous temperature and velocity at 1000m depth after one year integration in experiment CHANNEL-3. Every second velocity grid point is displayed and the colour shading ranges from 2^oC to 12^oC 29

2 Upper row: Streamfunction for the total flow in the classical TEM (a) in m^2/s, in the TEM-A (b) and in the TEM-D (c) in experiment CHANNEL-3. Contour interval is $1\,m^2/s$. Also shown are contours of $\bar{b}$ (red lines). Lower row: Eddy induced diffusivity K in cm^2/s in the classical TEM (d), in the TEM-A (e) and in the TEM-D (f). . . . 30

3 Same as in Fig. 2 but for experiment CHANNEL-12. 31

4 Same as in Fig. 3 but for experiment CHANNEL-12. 32

5 Eddy induced diffusivity K in cm^2/s in the TRM-G calculated to first order (a), second order (b), third order (c) and 4.th order (d). Note that (a) is the same as K in the TEM-G and (b) the same as K in the TEM-M. 33

6 Residual streamfunction in m^2/s in the TRM-G calculated to first order (a), second order (b), third order (c) and 4.th order (d). Contour interval is $1\,m^2/s$. 34

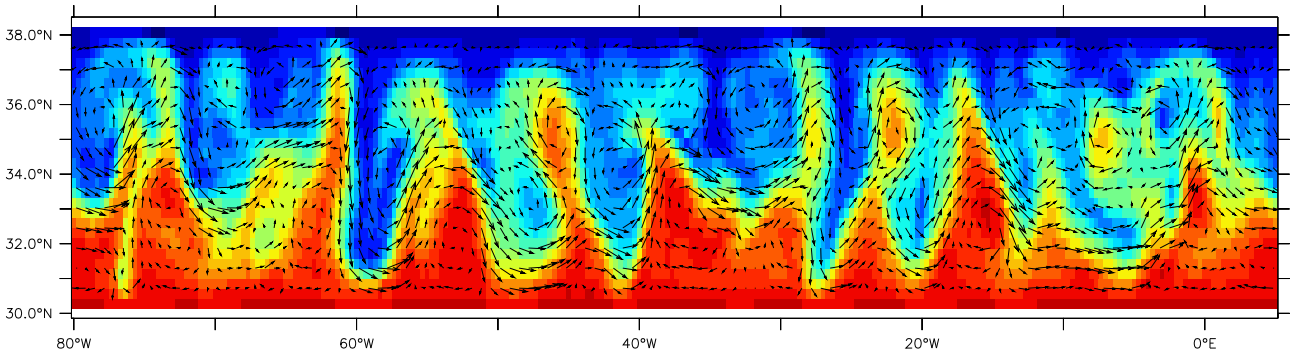

Figure 1: Instantaneous temperature and velocity at 1000m depth after one year integration in experiment CHANNEL-3. Every second velocity grid point is displayed and the colour shading ranges from 2^oC to 12^oC

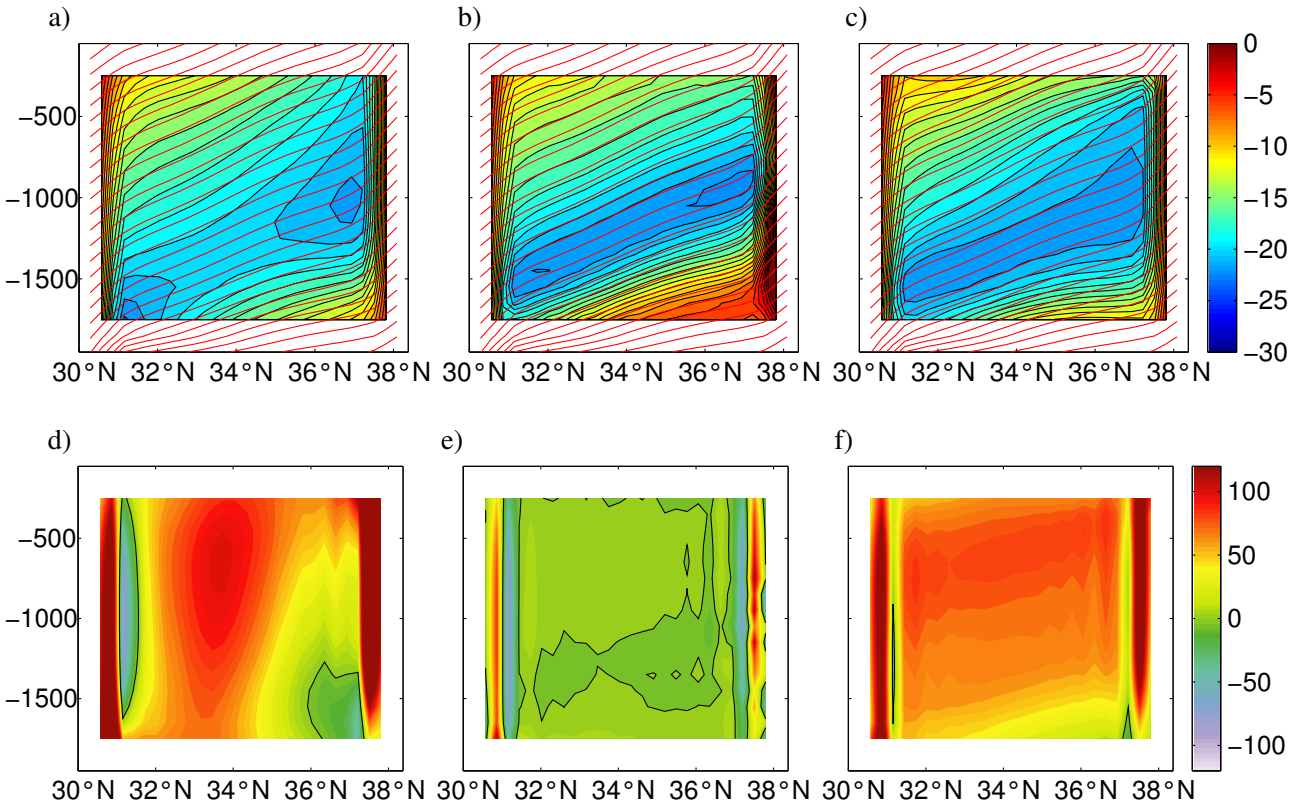

Figure 2: Upper row: Streamfunction for the total flow in the classical TEM (a) in m^2/s, in the TEM-A (b) and in the TEM-D (c) in experiment CHANNEL-3. Contour interval is $1\,m^2/s$. Also shown are contours of $\bar{b}$ (red lines). Lower row: Eddy induced diffusivity K in cm^2/s in the classical TEM (d), in the TEM-A (e) and in the TEM-D (f).

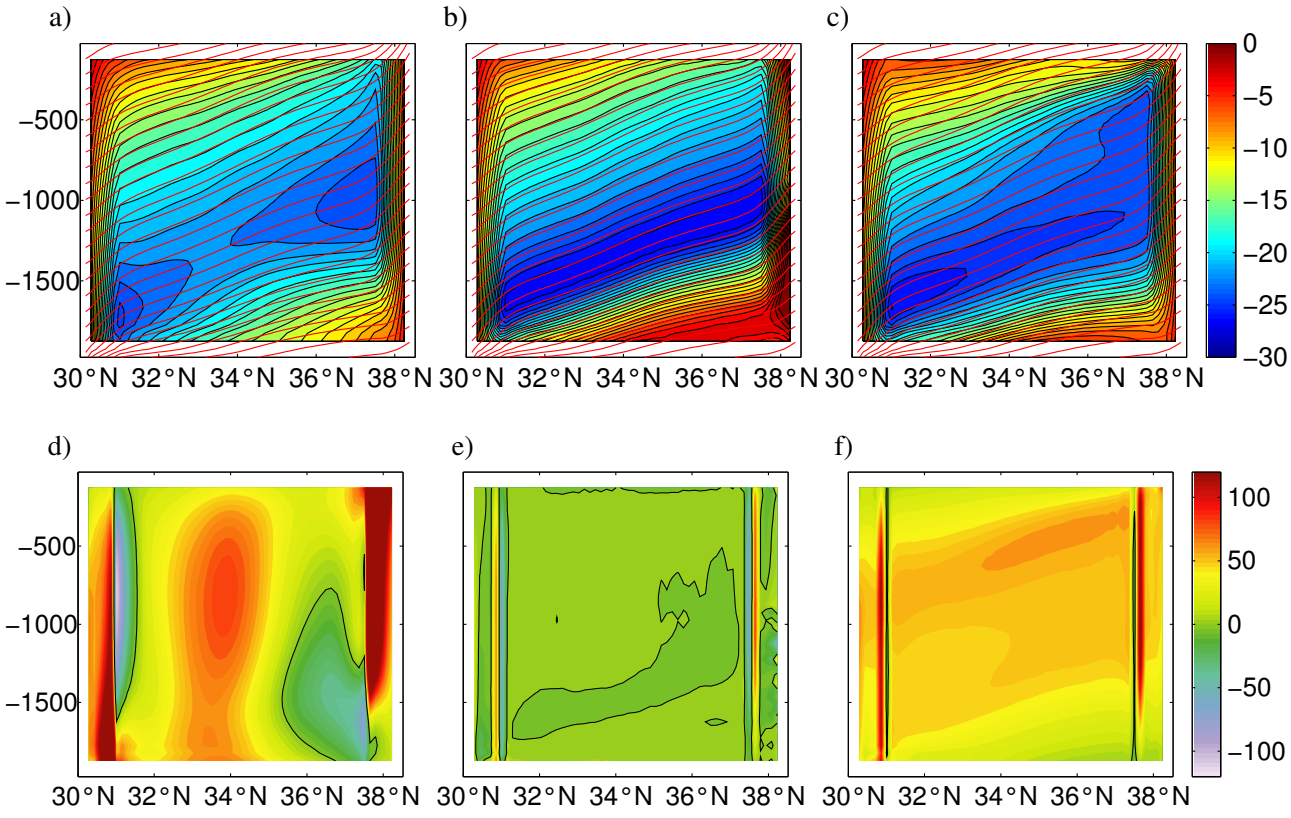

Figure 3: Same as in Fig. 2 but for experiment CHANNEL-12.

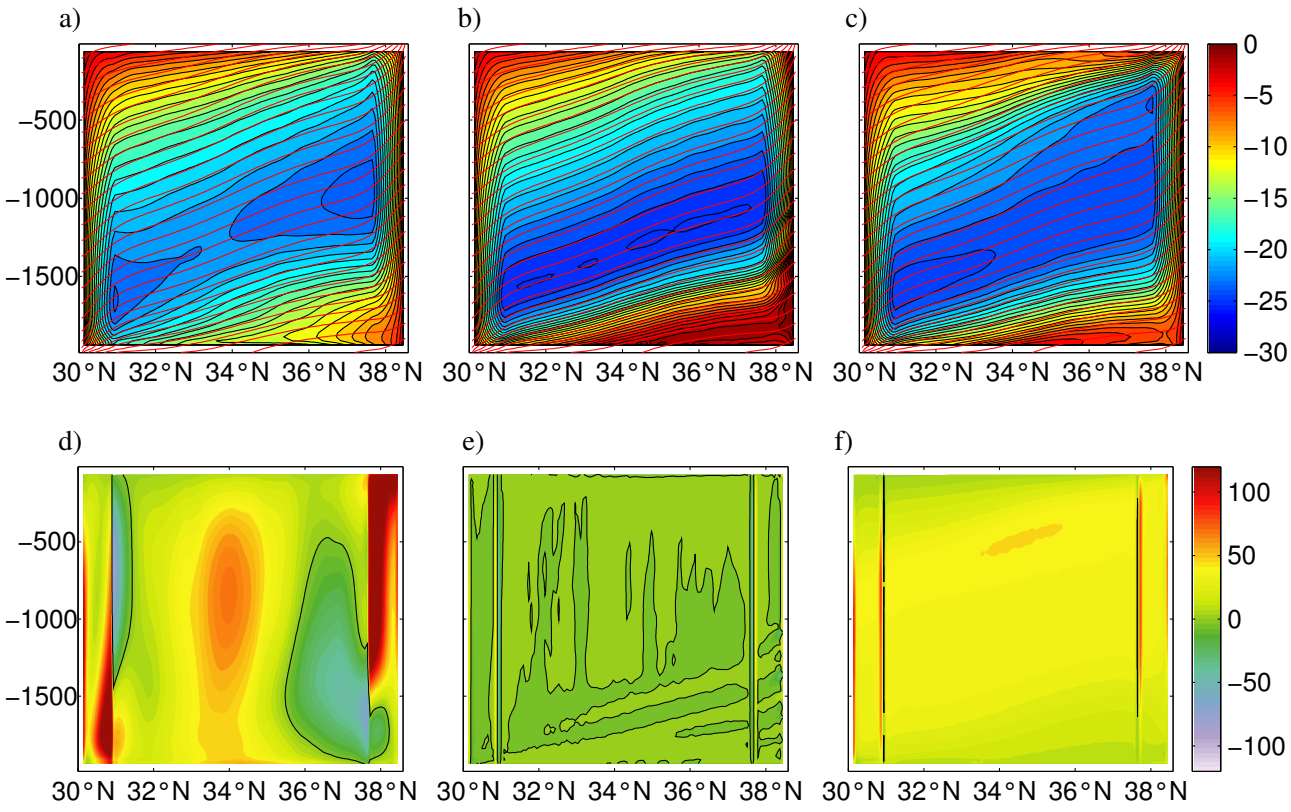

Figure 4: Same as in Fig. 3 but for experiment CHANNEL-12.

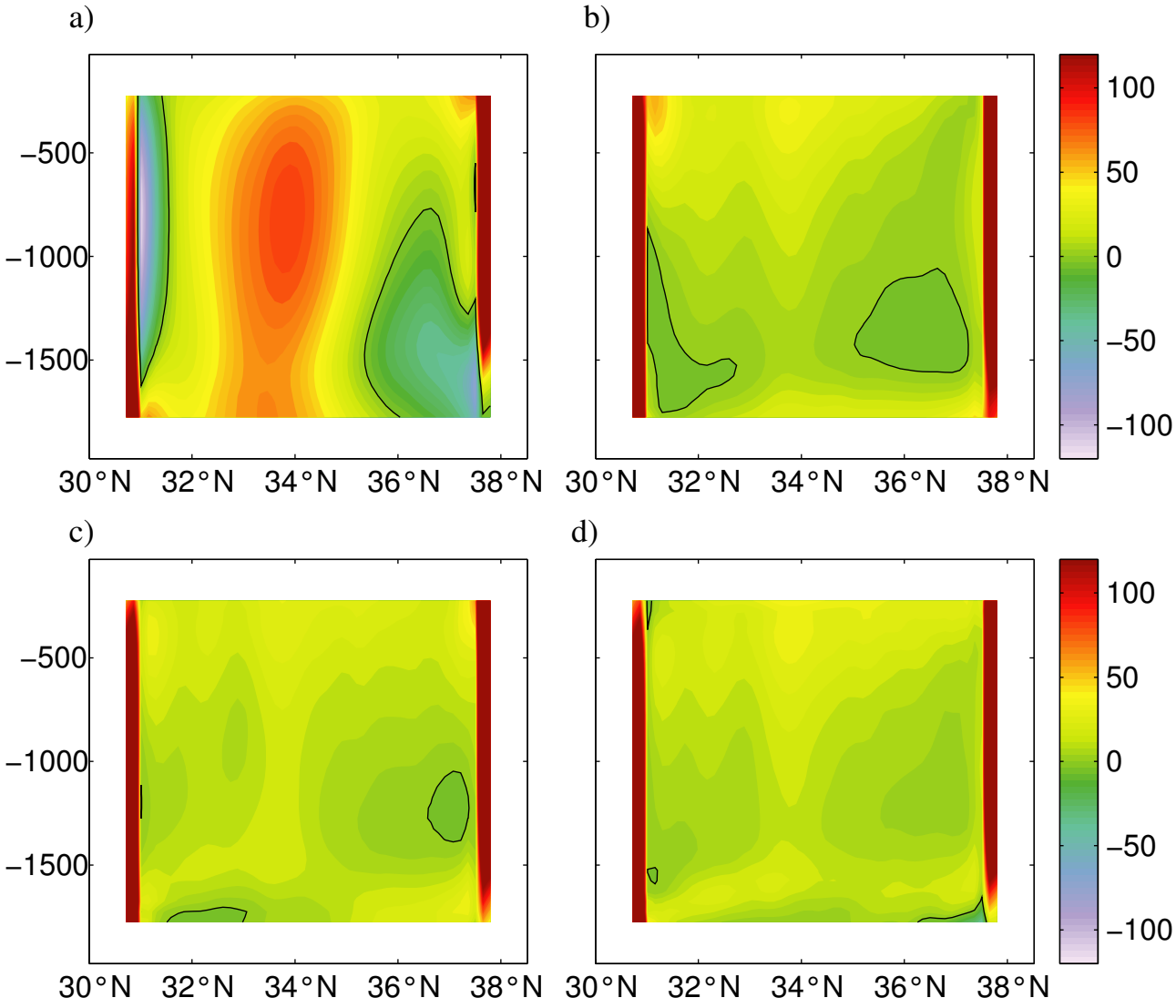

Figure 5: Eddy induced diffusivity K in cm^2/s in the TRM-G calculated to first order (a), second order (b), third order (c) and 4.th order (d). Note that (a) is the same as K in the TEM-G and (b) the same as K in the TEM-M.

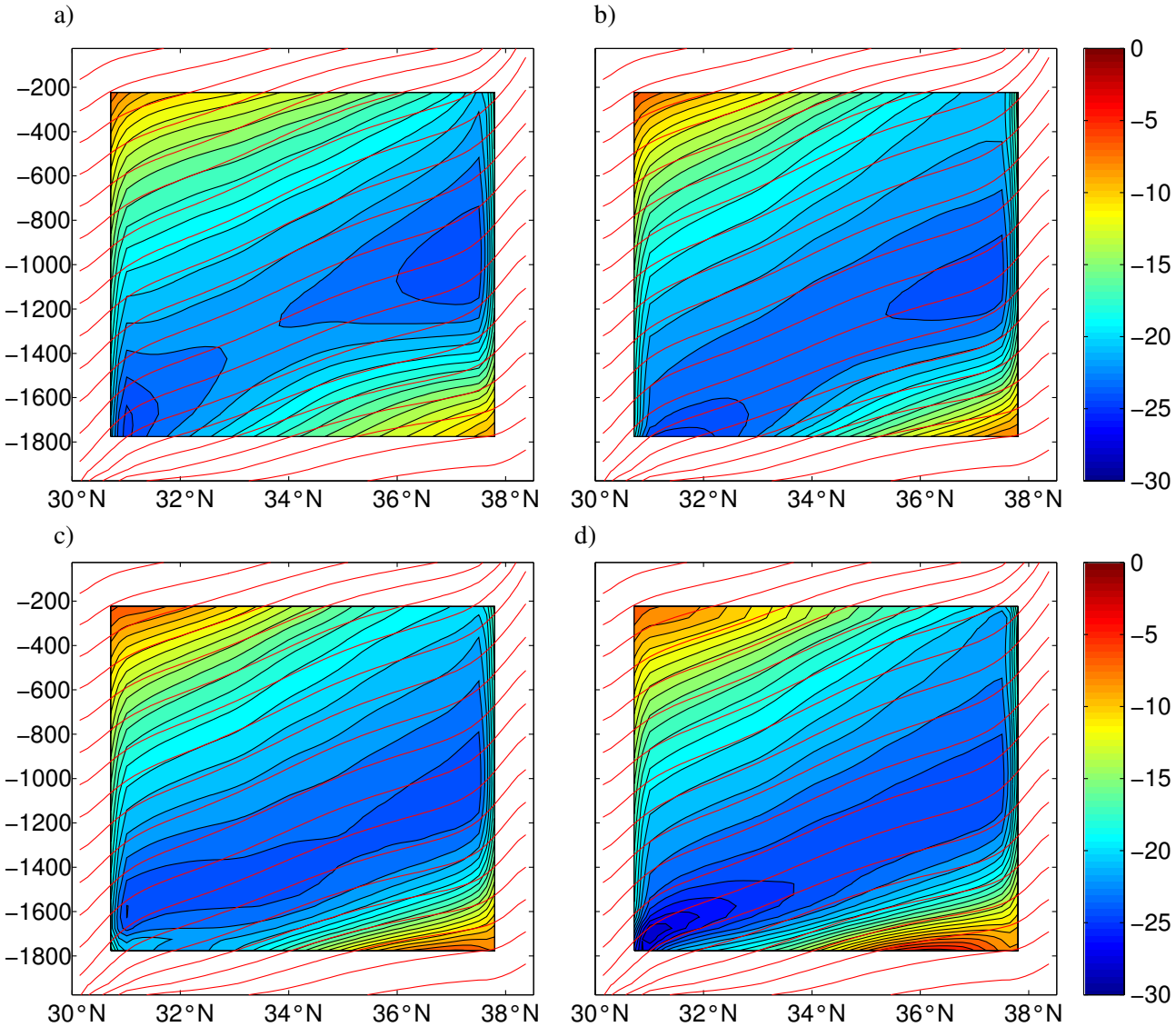

Figure 6: Residual streamfunction in m^2/s in the TRM-G calculated to first order (a), second order (b), third order (c) and 4.th order (d). Contour interval is $1\,m^2/s$.